

This is the accepted manuscript made available via CHORUS. The article has been published as:

# Quasiharmonic thermal elasticity of crystals: An analytical approach

Zhongqing Wu and Renata M. Wentzcovitch

Phys. Rev. B **83**, 184115 — Published 25 May 2011

DOI: [10.1103/PhysRevB.83.184115](https://doi.org/10.1103/PhysRevB.83.184115)

# Quasiharmonic thermal elasticity of crystals: an efficient analytical approach

Zhongqing Wu<sup>1,2\*</sup> and Renata. M. Wentzcovitch<sup>1</sup>

<sup>1</sup>Department of Chemical Engineering and Materials Science and  
Minnesota Supercomputing Institute, University of Minnesota, Minneapolis, MN 55455,  
USA

<sup>2</sup>School of Earth and Space Sciences, University of Science and Technology of China, Hefei,  
Anhui 230026, China

First principles quasiharmonic calculations play a very important role in mineral physics because they can predict the structural and thermodynamic properties of materials at pressure and temperature conditions of the Earth's interior that are still challenging for experiments. They also enable calculations of thermal elastic properties by providing second-order derivatives of free energies with respect to strain. The latter are essential to interpret seismic tomography of the mantle in terms of temperature, composition, and mineralogy, in the context of geophysical processes. However, these are exceedingly demanding computations requiring up to  $\sim 10^3$  parallel jobs running on tens or more processors each. Here we introduce an analytical and computationally simpler approach that requires only calculations of static elastic constants and phonon density of states for unstrained configurations. This approach, currently implemented for crystals with up to orthorhombic symmetry, decreases the computational effort, i.e., CPU time and human labor, by up to two orders of magnitude. Results for the major mantle phases periclase, MgO, and forsterite,  $\alpha$ -Mg<sub>2</sub>SiO<sub>4</sub>, show excellent agreement with previous first-principles results and experimental data.

Corresponding author, [wuzq10@ustc.edu.cn](mailto:wuzq10@ustc.edu.cn).

## 1. Introduction

Elasticity is a basic materials property essential to important phenomena such as propagation of elastic waves, flexure, brittle failure, etc. Elasticity of Earth forming minerals at high pressures and temperatures is a central topic in solid Earth geophysics. Seismic tomography is the primary source of information about Earth's interior. Interpretation of seismic observations in terms of mineralogical, compositional, and thermal fields requires basic knowledge of the elastic properties of minerals at relevant pressure and temperature conditions. Although experimental progress in the determination of elastic constants has been steady,<sup>1-3</sup> measurement of elastic constant at pressures and temperatures of the Earth's deep mantle and core (e.g., combined  $P > 50$  GPa and  $T > 2300$  K) remains a considerable challenge.

Finite strain theory allows one to express elastic moduli as a power series of strains similarly to an equation of state.<sup>4, 5</sup> These equations allow for extrapolations of elastic moduli from low to high pressures. This approach has been used to extrapolate bulk and shear moduli<sup>6-8</sup> and all elastic moduli.<sup>9, 10</sup> These equations are non-linear and quite sensitive to parameters that can cause large discrepancies in the elastic moduli in the extrapolated regime and must be used carefully with associated uncertainties. Experimental and theoretical elastic moduli in wide pressure ranges are still desirable to reevaluate these parameters in wider range of conditions.

First principles calculations of elastic moduli at planetary interior conditions can be obtained by quasiharmonic theory (QHA)<sup>11-13</sup> or by molecular dynamics(MD).<sup>14</sup> These approaches are complementary, with the QHA being essential below the Debye temperature and MD necessary near and above melting temperatures. At mantle temperatures and pressures both approaches have excellent predictive power and give similar results, except for systems stabilized by anharmonic fluctuations, such as  $\text{CaSiO}_3$ -perovskite.<sup>15-17</sup> The QHA, in particular,

gives the components of the elastic constant tensor in a continuum of pressures and temperatures. Therefore, QHA gives especially accurate temperature and pressure gradients of the elastic moduli. Although this approach is computationally less demanding than MD, it is still computationally very intensive, since it requires calculations of the vibrational density of state (VDoS) for each strained atomic configuration.<sup>11, 12</sup> It is, however, very labor intensive. For example, for an orthorhombic crystal with nine elastic constants, a very common symmetry in mineral structures, the calculation requires computations of VDoSs (at least 6 q-points to be used for interpolation in finer q-point meshes) for approximately 15 strained structures, in addition to the equilibrium structures, at several volumes ( $\sim 10$ ). The resulting workflow involves  $\sim 1,000$  parallel jobs divided in three stages, with output of each stage used as input to the next. This job deluge makes these calculations challenging to single researchers and prone to human error. A special cyber-infrastructure has been developed to manage these high temperature workflows by automatically dispatching jobs in distributed computational environments.<sup>18, 19</sup>

Here we introduce an approach that avoids calculations of VDoS for the strained configurations and reduces substantially computational requirement and labor. The former is approximately the same as that of calculations of thermal equations of state plus static elastic constants, which are performed routinely nowadays.

This paper is organized as follows: in section 2 we introduce the formalism; we briefly summarize the first principles method used and other details of the calculations in sections 3; section 4 illustrates the method's performance by comparing results on periclase, MgO, with previous results obtained by full QHA thermal elastic calculations.<sup>11</sup> Results on  $\alpha$ -Mg<sub>2</sub>SiO<sub>4</sub>, forsterite, the magnesium end-member of the major upper mantle phase, olivine, is also obtained and compared with experimental data in this section. Conclusions are presented in section 5.

## 2. Formalism

### 2.1 Quasiharmonic thermal elasticity

Isothermal elastic constants in Cartesian coordinates are given by:<sup>20</sup>

$$c_{ijkl}^T = \frac{1}{V} \left( \frac{\partial^2 F}{\partial e_{ij} \partial e_{kl}} \right) + \frac{1}{2} P (2\delta_{ij}\delta_{kl} - \delta_{il}\delta_{jk} - \delta_{ik}\delta_{jl}) \quad (1-1)$$

The relationship between isothermal and adiabatic elastic constants is<sup>5</sup>:

$$c_{ijkl}^S = c_{ijkl}^T + \frac{T}{VC_V} \frac{\partial S}{\partial e_{ij}} \frac{\partial S}{\partial e_{kl}} \delta_{ij} \delta_{kl} . \quad (1-2)$$

Here,  $e_{ij}$  ( $i=1-3$ ) are infinitesimal strains,  $C_V$  is heat capacity at constant volume,  $S$  is entropy, and

$F$  is the Helmholtz free energy, which is expressed in the QHA<sup>21, 22</sup> as:

$$F(e, V, T) = U_{st}(e, V) + \frac{1}{2} \sum_{q,m} \hbar \omega_{q,m}(e, V) + k_B T \sum_{q,m} \ln \{ 1 - \exp \left[ - \frac{\hbar \omega_{q,m}(e, V)}{k_B T} \right] \} \quad (2)$$

Subscript  $q$  is the phonon wave vector and  $m$  is the normal mode index.  $U_{st}(e, V)$  is the static internal energy at equilibrium volume  $V$  under isotropic pressure  $P$  with infinitesimal strain  $e$ .

$U_{st}(e, V)$  is computed by first principles here. As pointed out earlier<sup>11, 12, 23 24</sup> Eq (1.1) is equivalent to:

$$c_{ijkl}^T(P, T) = \frac{1}{V} \frac{\partial^2 G(e, P, T)}{\partial e_{ij} \partial e_{kl}} \bigg|_{P, T} \quad (3-1)$$

where  $G$  is the Gibbs free energy,

$$G = F + PV . \quad (3-2)$$

$P$  is also the trace of the stress tensor,

$$P = -\frac{1}{3} \sum_i \sigma_{ii}^T = -\frac{1}{3} \sum_i \frac{\partial F}{\partial e_{ii}} \bigg|_{P, T} \quad (3-3)$$

To compute  $c_{ijkl}^T(P, T)$ , the VDoS for equilibrium (unstrained) and deformed (strained) atomic configurations at selected pressures is necessary. In total these can number 100-200 configurations for orthorhombic structures, depending on the number of pressures ( $\sim 10$ ) and strains applied (15-20). First principles phonon calculations are much more time-consuming than standard self-consistent ones, e.g., two to three orders of magnitude, depending on the size of unit cell and the level of code parallelization. Therefore, calculation of thermal-elastic constants using the QHA is a relatively large computational effort and surely requires considerable man power.

The volume dependence of phonon frequencies contains also information about the strain dependence of phonon frequencies, especially for anisotropic crystals. If we are able to extract this frequency dependence under infinitesimal strains from its volume dependence, then we can obtain the thermal elastic constants without performing phonon calculations for strained configurations. Here we derive relations and formulas needed in calculating 9 elastic constants for orthorhombic crystals. The ideas used here can be applied to other crystals besides cubic, tetragonal, and orthorhombic crystals. But the new formulas are needed to calculate remaining elastic constants

## 2.2. Relations between volume and strain Grüneisen parameters for longitudinal strains

Mode Grüneisen parameters express the volume dependence of phonon frequencies:

$$\frac{d\omega_{qm}}{\omega_{qm}} = -\gamma_{qm} \frac{dV}{V} \quad (4-1)$$

The anisotropic generalization is:

$$\frac{\partial \omega_{qm}}{\omega_{qm}} = -\gamma_{qm}^{ij} e_{ij} \quad (4-2)$$

Henceforth we refer to  $\gamma_{qm}$  as *volume Grüneisen parameters* and to  $\gamma_{qm}^{ij}$  as *strain Grüneisen parameter*. If volume changes are caused exclusively by infinitesimal longitudinal strains, as in the case of orthorhombic crystals under hydrostatic compression, frequencies change as:

$$\frac{d\omega_{qm}}{\omega_{qm}} = -(\gamma_{qm}^{11}e_{11} + \gamma_{qm}^{22}e_{22} + \gamma_{qm}^{33}e_{33}) \quad (5)$$

Now, we can either express frequency changes as a power series in volume changes or as a power series on strains. To second order, the former is:

$$\begin{aligned} \Delta\omega_{qm} &= \frac{\partial\omega_{qm}}{\partial V} \cdot dV + \frac{1}{2} \frac{\partial^2\omega_{qm}}{\partial V^2} \cdot dV^2 \\ &= -\gamma_{qm}\omega_{qm}[e_{11} + e_{22} + e_{33} - (e_{11}^2 + e_{22}^2 + e_{33}^2)/2] \\ &\quad - \frac{1}{2}V \frac{\partial\gamma_{qm}}{\partial V} \omega_{qm} (e_{11} + e_{22} + e_{33})^2 \\ &\quad + \frac{1}{2}\gamma_{qm}^2\omega_{qm} (e_{11} + e_{22} + e_{33})^2 \end{aligned} \quad (6)$$

while the latter is:

$$\begin{aligned} \Delta\omega_{qm} &= \sum_i \frac{\partial\omega_{qm}}{\partial e_{ii}} \cdot e_{ii} + \frac{1}{2} \sum_{i,j} \frac{\partial^2\omega_{qm}}{\partial e_{ii} \partial e_{jj}} \cdot e_{ii}e_{jj} \\ &= -\omega_{qm}(\gamma_{qm}^{11}e_{11} + \gamma_{qm}^{22}e_{22} + \gamma_{qm}^{33}e_{33} - \frac{1}{2}\gamma_{qm}^{11}e_{11}^2 - \frac{1}{2}\gamma_{qm}^{22}e_{22}^2 - \frac{1}{2}\gamma_{qm}^{33}e_{33}^2) \\ &\quad - \frac{1}{2}\omega_{qm}(\frac{\partial\gamma_{qm}^{11}}{\partial e_{11}}e_{11}^2 + \frac{\partial\gamma_{qm}^{22}}{\partial e_{22}}e_{22}^2 + \frac{\partial\gamma_{qm}^{33}}{\partial e_{33}}e_{33}^2 + \frac{2\partial\gamma_{qm}^{11}}{\partial e_{12}}e_{11}e_{22} + \frac{2\partial\gamma_{qm}^{22}}{\partial e_{23}}e_{22}e_{33} + \frac{2\partial\gamma_{qm}^{33}}{\partial e_{31}}e_{33}e_{11}) \\ &\quad + \frac{1}{2}\omega_{qm}[(\gamma_{qm}^{11})^2e_{11}^2 + (\gamma_{qm}^{22})^2e_{22}^2 + (\gamma_{qm}^{33})^2e_{33}^2 + 2\gamma_{qm}^{11}\gamma_{qm}^{22}e_{11}e_{22} + 2\gamma_{qm}^{22}\gamma_{qm}^{33}e_{22}e_{33} + 2\gamma_{qm}^{33}\gamma_{qm}^{11}e_{33}e_{11}] \end{aligned} \quad (7)$$

For any combination of longitudinal strains, both equations must give the same frequency change.

Equating the first order terms in Eqs. (6) and (7) we get:

$$\gamma_{qm}^{11} \frac{e_{11}}{(e_{11} + e_{22} + e_{33})} + \gamma_{qm}^{22} \frac{e_{22}}{(e_{11} + e_{22} + e_{33})} + \gamma_{qm}^{33} \frac{e_{33}}{(e_{11} + e_{22} + e_{33})} = \gamma_{qm} \quad (8-1)$$

This relation also ensures that the last terms in Eqs. (6) and (7) are equal. To keep the second terms in the r.h.s. of Eqs. (6) and (7) equal, the corresponding coefficients in both equations should be related as:

$$\gamma_{qm}^2 \frac{\partial \gamma_{qm}^{jj}}{\partial e_{jj}} = \gamma_{qm}^{ji} \gamma_{qm}^{ij} V \frac{\partial \gamma_{qm}}{\partial V} \quad (8-2)$$

We now introduce two parameters  $\theta_{qm}$  and  $\phi_{qm}$ , which we call the *Grüneisen azimuth angles* (see Fig. 1) for each phonon  $(q, m)$ . They are defined in relation to Eq. (8-1) as:

$$\begin{aligned} \gamma_{qm}^{11} &= \frac{e_{11} + e_{22} + e_{33}}{e_{11}} \gamma_{qm} \cos^2 \theta_{qm} \sin^2 \phi_{qm} \\ \gamma_{qm}^{22} &= \frac{e_{11} + e_{22} + e_{33}}{e_{22}} \gamma_{qm} \sin^2 \theta_{qm} \sin^2 \phi_{qm} \\ \gamma_{qm}^{33} &= \frac{e_{11} + e_{22} + e_{33}}{e_{33}} \gamma_{qm} \cos^2 \phi_{qm} \end{aligned} \quad (9)$$

They are simple auxiliary quantities and express the sensitivity of strain Grüneisen parameters to strains. We introduce a distribution function  $f(\theta, \phi)$ , defining the density of modes with Grüneisen azimuth angles between  $(\theta, \phi)$  and  $(\theta + d\theta, \phi + d\phi)$ . For isotropic materials  $f(\theta, \phi)$  must be a constant:

$$f = \frac{3N}{4\pi}, \quad (10)$$

where  $3N$  is the total numbers of modes. This is not the case for anisotropic materials but we will assume this isotropic distribution of Grüneisen azimuth angles. This approximation is equivalent to having a completely isotropic material from the thermal point of view, and therefore isotropic thermal pressure. It is well known that thermal pressure is not isotropic,<sup>25</sup> however, treatment of thermal pressure as isotropic does not incur in significant errors in elastic constants at mantle conditions.<sup>26</sup> As will be seen later, this approximation works very well up to very high temperatures.

As will be shown in the next section, calculations of thermal elastic properties require average values of strain Grüneisen parameters, of their products, or of their strain derivatives. We obtain



these averages from Eqs. (8) - (10) and by assuming a single average value for the volume Grüneisen parameter:

$$\bar{\gamma} = \frac{1}{3N} \sum_{qm} \gamma_{qm} \quad (11-1)$$

$$\begin{aligned} \overline{\gamma^{11}} &= \frac{e_{11} + e_{22} + e_{33}}{e_{11}} \bar{\gamma} \frac{\int_{\phi=0}^{\pi} \int_{\theta=0}^{2\pi} f \cos^2 \sin^3 \phi d\phi d\theta}{\int_{\phi=0}^{\pi} \int_{\theta=0}^{2\pi} f \sin \phi d\phi d\theta} \\ &= \frac{e_{11} + e_{22} + e_{33}}{3e_{11}} \bar{\gamma} \end{aligned} \quad (11-2)$$

The averages necessary to compute thermal elastic constants are:

$$\overline{\gamma^{ii}} = \frac{e_{11} + e_{22} + e_{33}}{3e_{ii}} \bar{\gamma} \quad (12-1)$$

$$\overline{\gamma^{ii} \gamma^{jj}} = \begin{cases} \frac{1}{5} \frac{(e_{11} + e_{22} + e_{33})^2}{e_{ii} e_{jj}} \overline{(\gamma)^2} & \text{if } i = j \\ \frac{1}{15} \frac{(e_{11} + e_{22} + e_{33})^2}{e_{ii} e_{jj}} \overline{(\gamma)^2} & \text{if } i \neq j \end{cases} \quad (12-2)$$

where

$$\overline{(\gamma)^2} = \frac{1}{3N} \sum_{qm} \gamma_{qm}^2 \quad (12-3)$$

From Eqs. (8-2), (12-1), and (12-2) we also get

$$\frac{\overline{\gamma^{ii}}}{\partial e_{jj}} = \begin{cases} \frac{1}{5} \frac{(e_{11} + e_{22} + e_{33})^2}{e_{ii} e_{jj}} V \frac{\partial \gamma}{\partial V} & \text{if } i = j \\ \frac{1}{15} \frac{(e_{11} + e_{22} + e_{33})^2}{e_{ii} e_{jj}} V \frac{\partial \gamma}{\partial V} & \text{if } i \neq j \end{cases} \quad (12-4)$$

where

$$\overline{V \frac{\partial \gamma}{\partial V}} = \frac{1}{3N} \sum_{qm} V \frac{\partial \gamma_{qm}}{\partial V} \quad (12-5)$$

In all cases  $i,j=1-3$ .

Since  $\gamma_{qm}$ , their volume derivatives, and their averages are obtained at various volumes (pressures), average strain Grüneisen parameters and the average of their products or strain derivatives shown in Eqs. (12-1,2,3) can be obtained as well, avoiding a direct calculation of phonon frequency changes with strains. As will be seen below, despite the approximations involved, there appears to be an advantage to this scheme.

### 2.3. Thermal elastic constants

#### 2.3.1. Longitudinal and off-diagonal elastic constant

Orthorhombic crystals have nine elastic constants. With exception of the shear elastic constant in Eq. (1) the others can be written as:

$$c_{ijj}^T(V, T) = \frac{1}{V} \left( \frac{\partial^2 F(\mathbf{e}, V, T)}{\partial e_{ii} \partial e_{jj}} \right) + (1 - \delta_{ij}) P(V, T) = c_{ijj}^{st}(V) + c_{ijj}^{ph}(V, T) \quad (13)$$

where  $i,j = 1-3$ .  $c_{ijj}^T(P, T)$  is then obtained by interchanging  $V(P, T)$  by  $P(V, T)$  above.

$$c_{ijj}^{st}(V) = \left( \frac{\partial^2 U_{st}}{\partial e_{ii} \partial e_{jj}} \right) + (1 - \delta_{ij}) P^{st}(V) \quad (14-1)$$

is the static elastic constant with  $P^{st}(V) = -\partial U_{st}(V) / \partial V$ , the static pressure. Phonon contributions to the elastic constants are included in the second term:

$$c_{ijj}^{ph}(V, T) = c_{ijj}^{zpm}(V) + c_{ijj}^{th}(V, T) + (1 - \delta_{ij}) P^{ph}(V, T) \quad (14-2)$$

where  $P^{ph}(V, T) = P(V, T) - P^{st}(V)$  is the contribution of vibrations to pressure. Zero point motion and thermal contributions to the elastic constants are given by:

$$c_{ijij}^{zpm}(V) = \frac{\hbar}{2V} \sum_{qm} \left( \frac{\partial^2 \omega_{qm}(V)}{\partial e_{ii} \partial e_{jj}} \right) = \frac{\hbar}{2V} \sum_{qm} \left( \gamma_{qm}^{ii} \gamma_{qm}^{jj} - \frac{\partial \gamma_{qm}^{ii}}{\partial e_{jj}} + \delta_{ij} \gamma_{qm}^{ii} \right) \omega_{qm} \quad (15-1)$$

$$\begin{aligned} c_{ijij}^{th}(V, T) &= \frac{k_B T}{V} \sum_{qm} \frac{\partial^2 [\ln(1 - e^{-Q_{qm}})]}{\partial e_{ii} \partial e_{jj}} \\ &= \frac{k_B T}{V} \sum_{qm} \left[ -Q_{qm}^2 \cdot \frac{e^{Q_{qm}}}{(e^{Q_{qm}} - 1)^2} \cdot \gamma_{qm}^{ii} \gamma_{qm}^{jj} + \frac{e^{Q_{qm}}}{(e^{Q_{qm}} - 1)} \left( \gamma_{qm}^{ii} \gamma_{qm}^{jj} - \frac{\partial \gamma_{qm}^{ii}}{\partial e_{jj}} + \gamma_{qm}^{ii} \delta_{ij} \right) \right] \end{aligned} \quad (15-2)$$

where  $Q_{qm} = \hbar \omega_{qm} / k_B T$ . At this point we replace  $\gamma_{qm}^{ii}$ ,  $\gamma_{qm}^{jj}$ , and  $\frac{\partial \gamma_{qm}^{ii}}{\partial e_{jj}}$  by their averages over 3N modes, as in Eqs. (11-1, 12-3, and 12-5). We also verify that  $Q_{qm}^2 e^{Q_{qm}} / (e^{Q_{qm}} - 1)^2$  and  $Q_{qm} / (e^{Q_{qm}} - 1)$  are close to 1, above room temperatures. Then we have

$$c_{ijij}^{zpm}(V) = \frac{3N\hbar}{2V} \left( \overline{\gamma^{ii} \gamma^{jj}} - \overline{\frac{\partial \gamma^{ii}}{\partial e_{jj}}} + \delta_{ij} \overline{\gamma^{ii}} \right) \overline{\omega} \quad (16-1)$$

$$c_{ijij}^{th}(V, T) = \frac{3Nk_B T}{V} \left[ -\overline{Q_{qm}^2 \cdot \frac{e^{Q_{qm}}}{(e^{Q_{qm}} - 1)^2} \cdot \gamma^{ii} \gamma^{jj}} + \overline{\frac{e^{Q_{qm}}}{(e^{Q_{qm}} - 1)} \left( \gamma^{ii} \gamma^{jj} - \frac{\partial \gamma^{ii}}{\partial e_{jj}} + \gamma^{ii} \delta_{ij} \right)} \right] \quad (16-2)$$

Similarly, the derivative of the entropy with respect to strain, which is needed to calculate adiabatic elastic constants (Eq. 1), is

$$\frac{\partial S}{\partial e_{ii}} = k_B \sum_{qm} Q_{qm}^2 \frac{e^{Q_{qm}}}{(e^{Q_{qm}} - 1)^2} \gamma_{qm}^{ii} = 3Nk_B \overline{Q_{qm}^2 \frac{e^{Q_{qm}}}{(e^{Q_{qm}} - 1)^2} \gamma^{ii}} \quad (17)$$

### 2.3.2 Shear elastic constants

Similarly, shear elastic constants can be expressed as

$$c_{ijij}^T = c_{ijij}^{st} + c_{ijij}^{ph} \quad (18)$$

where  $i \neq j = 1, 2, 3$ . So far, the second term in Eq. (18) is unknown. Fig. 2 shows strains depicted in two coordinate systems. The equation relating Cartesian strains  $\mathbf{e}$  and  $\mathbf{e}'$  in coordinate systems rotated by an angle  $\theta$  in the  $X_1X_2$  plane is:

$$\mathbf{e}' = \mathbf{T}^{-1} \mathbf{e} \mathbf{T} \quad (19)$$

where

$$\mathbf{T} = \begin{bmatrix} \cos \theta & -\sin \theta & 0 \\ \sin \theta & \cos \theta & 0 \\ 0 & 0 & 1 \end{bmatrix}. \quad (20)$$

In particular, for  $\theta = \pi/4$  shear strain in coordinate system  $\mathbf{X}$  transforms to pure diagonal strains in coordinate  $\mathbf{X}'$ , irrespective of crystal symmetry:

$$\begin{bmatrix} 0 & e & 0 \\ e & 0 & 0 \\ 0 & 0 & 0 \end{bmatrix}_{\mathbf{X}} \rightarrow \begin{bmatrix} e & 0 & 0 \\ 0 & -e & 0 \\ 0 & 0 & 0 \end{bmatrix}_{\mathbf{X}'}. \quad (21)$$

Such coordinate transformation does not change the strain energy, namely,

$$\frac{1}{2} (c_{ijkl}^{st} + c_{ijkl}^{ph}) e_{ij} e_{kl} = \frac{1}{2} (c_{i'j'k'l'}^{st} + c_{i'j'k'l'}^{ph}) e_{i'j'} e_{k'l'} \quad (22)$$

The static elastic constant cancels because this relationship is true also for the static part. Therefore, the total phonon contribution to shear elastic constants can be expressed as:

$$c_{ijij}^{ph} = (c_{i'j'j'j'}^{ph} + c_{j'j'j'j'}^{ph} - 2c_{i'i'j'j'}^{ph})/4 \quad (23)$$

Eqs (12) is derived for arbitrary Cartesian coordinate system if Eq. (10) is a good approximation under the corresponding diagonal strains and hence can be used to calculate all terms in the r.h.s. of Eqs (23). The difference is that we need to know the corresponding strains in the  $\mathbf{X}'$  coordinate system caused by hydrostatic compression. Since

$$\begin{bmatrix} e_{11} & 0 & 0 \\ 0 & e_{22} & 0 \\ 0 & 0 & e_{33} \end{bmatrix}_{\mathbf{X}} \rightarrow \begin{bmatrix} (e_{11} + e_{22})/2 & (e_{11} - e_{22})/2 & 0 \\ (e_{11} - e_{22})/2 & (e_{11} + e_{22})/2 & 0 \\ 0 & 0 & e_{33} \end{bmatrix}_{\mathbf{X}'}, \quad (24)$$

we have:

$$e_{1'1'} = \frac{e_{11} + e_{22}}{2}; e_{2'2'} = \frac{e_{11} + e_{22}}{2}; e_{3'3'} = e_{33}; e_{1'2'} = \frac{e_{11} - e_{22}}{2} \quad (25)$$

Here we take  $e_{1'2'}$  as negligible and we are left only with pure longitudinal strains  $e_{i'1'}$  ( $i'=1,3$ ) mentioned above in  $\mathbf{X}'$  system. For diagonal strains, Eq. (12) is applicable and we only need to replace  $e_{11}$ ,  $e_{22}$  and  $e_{33}$  by  $e_{1'1'}$ ,  $e_{2'2'}$  and  $e_{3'3'}$  to obtain  $c_{i'i'j'j'}^{ph}$ . We also need new mode Grüneisen parameters,  $\gamma'_{qm}$ , corresponding to these longitudinal strain. However, the difference between  $\gamma'_{qm}$  and  $\gamma_{qm}$  should be small because (i) in contrast to the longitudinal strain, the shear strain  $e_{1'2'}$  is small (see Eq. (25), it is 0 for cubic systems), and (ii) frequency changes caused by the shear strain are far smaller than the frequency changes caused by the longitudinal strain hence contribution to Grüneisen parameters from the small shear strain in Eq. (25) are relatively small. Therefore, it is reasonable to use the same  $\gamma_{qm}$  to calculate shear elastic constants without sacrificing much accuracy. We then obtain all  $c_{i'i'j'j'}^{ph}$  necessary to calculate  $c_{ijij}$  in Eq. (23). For example, formula (12-1) in the  $\mathbf{X}'$  coordinate system changes into:

$$\overline{\gamma^{1'1'}} = \frac{2(e_{11} + e_{22} + e_{33})}{3(e_{11} + e_{22})} \overline{\gamma} \quad (26)$$

where  $e_{11}$ ,  $e_{22}$ , and  $e_{33}$  are strains in  $\mathbf{X}$  caused by hydrostatic compression. For cubic crystals,  $e_{11} = e_{22} = e_{33}$ ,  $c_{1'1'1'1'}^{ph} = c_{1111}^{ph}$ ,  $c_{1'1'2'2'}^{ph} = c_{1122}^{ph}$ , and  $c_{1212}^{ph} = (c_{1111}^{ph} - c_{1122}^{ph})/2$ , the latter being a well known result that holds for isotropic systems.

### 3. Calculation method

### 3.1 First principles approach

Calculations were performed using the Quantum ESPRESSO<sup>27</sup> suite of codes for electronic structure calculations based on density functional theory, plane waves,<sup>28</sup> and pseudopotentials. The local-density approximation<sup>29, 30</sup> is used in all calculations. The pseudopotential for magnesium was generated by the method of von Barth and Car, while those for oxygen and silicon were generated by the method of Troullier and Martins.<sup>31</sup> The plane wave cutoff energy is 70 Ry. Brillouin-zone sampling for electronic states was carried out on 10 and 4 special  $k$ -points for periclase (2 atoms/cell) and forsterite (28 atoms/cell), respectively. Structural optimizations were carried out using damped variable cell shape molecular dynamics.<sup>32</sup> The VDoSs of periclase and forsterite used in this work were previously calculated by Wu et al<sup>33</sup> and Yu et al<sup>34</sup> using density functional perturbation theory (DFPT).<sup>35</sup>

### 3.2 Other details

The calculations were repeated for 8 to 10 pressures. The volume dependence of the free energy, lattice parameters, and phonon frequencies were fitted using polynomials to third power in Eulerian strains. Linear compressions were obtained in points of a regular grid in Eulerian strain, i.e.,  $\frac{\Delta a}{a} : \frac{\Delta b}{b} : \frac{\Delta c}{c} = e_{11} : e_{22} : e_{33}$ , and were then used in Eqs. (12).

## 4. Results and discussion

Here we present the thermal elastic constants of two important Earth forming minerals, cubic MgO (periclase) and orthorhombic forsterite ( $\alpha$  phase of  $\text{Mg}_2\text{SiO}_4$ ). These are the magnesium end-members of ferropericlase, the second major phase of the lower mantle, and olivine, the most abundant phase of the upper mantle. The (adiabatic) thermal elastic constants<sup>11</sup> and thermodynamic properties<sup>36</sup> of MgO have been calculated by first principles within

quasiharmonic theory. Its thermal properties have also been calculated including anharmonic effects.<sup>33, 37</sup> Here we repeat the same static and high temperature elastic constant calculations. The quasiharmonic VDoS is the same one obtained in Ref.<sup>33</sup>. As shown in Fig. 3, the calculated elastic moduli of MgO at zero pressure are essentially identical to those predicted by the quasiharmonic method using strained configurations, except for some small deviations in  $c_{44}$  above 2000 K and  $c_{12}$  above 1200 K. In fact, present results on  $c_{11}$  and  $c_{12}$  appear to agree slightly better with the experimental values of Isaak et al.<sup>38</sup> than results obtained using strained configurations, while  $c_{44}$  appears to be quite comparable. Deviations of calculated  $c_{11}$  and  $c_{12}$  from the experimental data at high temperature are caused by the overestimation of the thermal expansivity predicted by the QHA.<sup>33, 37</sup> The discrepancy between theoretical and experimental  $c_{44}$  remains; its cause is unlikely to be unharmonicity since it is present even at room temperature.

Unexpectedly, the present method produces results slightly more consistent with experiments than the original method, especially the slope of  $c_{44}$ , despite the fact it appears to be more approximated. The reason of this unexpected result is that the present method does not use strained configurations to obtain the thermal contribution to the elastic constant. “Infinitesimal” strains in practice are small but non-vanishing, i.e.,  $< 1\%$ . Ideally one would like to perform calculations using even smaller strain amplitudes, e.g. 0.1%. However, the convergence criterion in the self-consistent cycle must decrease by a factor of ten for comparable accuracy in the static elastic constants and this is computationally costly. A 1% strain is a compromise between a small strain and good numerical accuracy for energy differences between strained configurations with a reasonable total energy convergence criterion. Although small, a 1% strain changes slightly the internal pressure at which elastic constants are reported. In the present approach, pressure is unaltered since no strains are applied in practice.

The (adiabatic) thermal elastic moduli of forsterite at zero pressure are also in very good agreement with experimental data (see Fig. 4). Only static elastic constants<sup>39</sup> and thermal properties<sup>40,34</sup> have been reported by first principles so far. At room temperature, the longitudinal elastic constants  $c_{11}$ ,  $c_{22}$  and  $c_{33}$  are slightly smaller than the experimental data.<sup>41</sup> However, their temperature derivatives are in excellent agreement with the experimental results. At temperatures above  $\sim 1000$  K, the longitudinal elastic constant decreases more slowly with temperature than the experimental data. This small difference in temperature gradient also appears in the adiabatic bulk modulus,  $K_S$ , (see Fig. 4). The bulk modulus in Fig. 4 was calculated from the equation of state without using any of the approximations mentioned above. Therefore, the deviation from experimental data must be attributed to the QHA as in the case of MgO. However, MgO and forsterite show opposite behavior. The longitudinal elastic constant of MgO decreases more rapidly than the experimental data, while those of forsterite decrease more slowly than the data. This different behavior is also consistent with the opposite effects caused by anharmonicity in these two minerals:<sup>37</sup> at high temperatures the QHA overestimates the thermal expansivity in MgO and underestimates the thermal expansivity in forsterite.<sup>37, 40</sup>

High-pressure results in forsterite also reproduce experimental data very well. Fig. 5 shows the pressure dependence of longitudinal ( $V_P$ ) and shear ( $V_S$ ) velocities in polycrystalline aggregates<sup>42</sup> of forsterite at various temperatures. Static calculations are in good agreement with previous results by da Silva *et al.*<sup>39</sup> and both overestimate longitudinal velocities. After inclusion of zero point motion and thermal effects, the agreement with experimental data<sup>41, 43, 44</sup> improves considerably at 300 K and 1070 K. The temperature effect on velocities, as expected, decreases with increasing pressure, e.g., from 0.47 (0.30) m/s/K at 0 GPa to 0.32 (0.19) m/s/K at 10 GPa for the longitudinal (shear) velocity. Given the overall agreement between calculations and



experiments at low pressures and high temperatures, the relatively small disagreement between theory and experiments at 1073 K between 5 and 8 GPa<sup>44</sup> is likely caused by difficulties in measuring shear velocities at high pressures and temperatures. In overall, the current method offers similar accuracy for cubic and orthorhombic systems.

#### 4. Summary and conclusions

We have introduced an efficient and effective method for calculating thermal elastic properties of crystals with up to orthorhombic symmetry at high pressures and temperatures. It combines static elastic constant calculations with quasiharmonic calculations of VDoS and free energies for structures under isotropic pressure only. In contrast with a previous method requiring free energy calculations for strained configurations,<sup>23</sup> the present method makes use of analytical expressions for the thermal part of the elastic constants relating strain derivatives (strain Grüneisen parameters) with volume derivatives of phonon frequencies (mode Grüneisen parameters). The central approximations used in the derivation of these relationships consist in assuming that the Grüneisen azimuth angles, which describe the relation between strain Grüneisen parameters and mode Grüneisen parameters, have isotropic distribution, which is equivalent to assuming that thermal pressure is isotropic.

The first principles implementation of this method has offered results in periclase (MgO) and forsterite ( $\alpha$ -Mg<sub>2</sub>SiO<sub>4</sub>) that are in excellent agreement with experimental data and with previous calculations of elastic constants in MgO at high pressures and temperatures. Since this method does not require calculations of VDoS for strained configurations, it requires 10-20 times less computations for orthorhombic systems. But, even more important, is the reduction of labor involved in preparing and monitoring  $\sim 10^3$  parallel jobs, as required by the previous approach.

## Acknowledgements

This work was supported by the National Science Foundation under grants NSF/EAR 0635990, NSF/ATM 0428774 (*VLab*), and NSF/EAR 1047629.

## References

- <sup>1</sup> B. Li and R. C. Liebermann, Proc. Natl. Acad. Sci. U. S. A. **104**, 9145 (2007).
- <sup>2</sup> M. Murakami, Y. Ohishi, N. Hirao, and K. Hirose, Earth Planet. Sci. Lett. **277**, 123 (2009).
- <sup>3</sup> D. Bass, S. V. Sinogikin, and B. S. Li, Elements **4**, 165 (2008).
- <sup>4</sup> L. Thomsen, J. Phys. Chem. Solids **33**, 363 (1972).
- <sup>5</sup> G. F. Davies, J. Phys. Chem. Solids **35**, 1513 (1974).
- <sup>6</sup> T. S. Duffy and D. L. Anderson, Journal of Geophysical Research-Solid Earth and Planets **94**, 1895 (1989).
- <sup>7</sup> B. R. Hacker, G. A. Abers, and S. M. Peacock, J. Geophys. Res. **108** (2003).
- <sup>8</sup> F. Cammarano, S. Goes, P. Vacher, and D. Giardini, Physics of the Earth and Planetary Interiors **138**, 197 (2003).
- <sup>9</sup> B. B. Karki, L. Stixrude, and R. M. Wentzcovitch, Reviews of Geophysics **39**, 507 (2001).
- <sup>10</sup> L. Stixrude and C. Lithgow-Bertelloni, Geophysical Journal International **162**, 610 (2005).
- <sup>11</sup> B. B. Karki, R. M. Wentzcovitch, S. de Gironcoli, and S. Baroni, Science **286**, 1705 (1999).
- <sup>12</sup> R. M. Wentzcovitch, B. B. Karki, M. Cococcioni, and S. de Gironcoli, Phys. Rev. Lett. **92** (2004).

- 13 R. M. Wentzcovitch, T. Tsuchiya, and J. Tsuchiya, Proc. Natl. Acad. Sci. U. S. A. **103**, 543 (2006).
- 14 A. R. Oganov, J. P. Brodholt, and G. D. Price, Nature **411**, 934 (2001).
- 15 L. Stixrude, R. E. Cohen, R. C. Yu, and H. Krakauer, Am. Mineral. **81**, 1293 (1996).
- 16 R. Caracas and R. M. Wentzcovitch, Acta Crystallographica Section B-Structural Science **62**, 1025 (2006).
- 17 L. Li, D. J. Weidner, J. Brodholt, D. Alfe, G. D. Price, R. Caracas, and R. Wentzcovitch, Physics of the Earth and Planetary Interiors **155**, 249 (2006).
- 18 C. R. S. da Silva, P. R. C. da Silveira, B. Karki, R. M. Wentzcovitch, P. A. Jensen, E. F. Bollig, M. Pierce, G. Erlebacher, and D. A. Yuen, Physics of the Earth and Planetary Interiors **163**, 321 (2007).
- 19 P. R. C. da Silveira, C. R. S. da Silva, and R. M. Wentwovitch, Comput. Phys. Commun. **178**, 186 (2008).
- 20 T. H. K. Barron and M. L. Klein, Proceedings of the Physical Society of London **85**, 523 (1965).
- 21 M. Born and K. Huang, *Dynamical Theory of Crystal Lattices* ( Oxford at the Clarendon Press, Hong Kong, 1956).
- 22 D. C. Wallace, *Thermodynamics of Crystals*. (John Wiley and Sons, New York, 1972).
- 23 R. M. Wentzcovitch, Z. Q. Wu, and P. Carrier, Theoretical and Computational Methods in Mineral Physics: Geophysical Applications **71**, 99 (2010).
- 24 G. J. Ackland and S. K. Reed, Phys. Rev. B **67** (2003).
- 25 P. Carrier, R. Wentzcovitch, and J. Tsuchiya, Phys. Rev. B **76**, 064116 (2007).
- 26 P. Carrier, J. F. Justo, and R. M. Wentzcovitch, Phys. Rev. B **78** (2008).

- 27 P. Giannozzi, et al., J. Phys.: Condens. Matter **21**, 395502 (2009).
- 28 J. Ihm, A. Zunger, and M. L. Cohen, Journal of Physics C-Solid State Physics **12**, 4409 (1979).
- 29 D. M. Ceperley and B. J. Alder, Phys. Rev. Lett. **45**, 566 (1980).
- 30 J. P. Perdew and A. Zunger, Phys. Rev. B **23**, 5048 (1981).
- 31 N. Troullier and J. L. Martins, Phys. Rev. B **43**, 1993 (1991).
- 32 R. M. Wentzcovitch, Phys. Rev. B **44**, 2358 (1991).
- 33 Z. Q. Wu, R. M. Wentzcovitch, K. Umemoto, B. S. Li, K. Hirose, and J. C. Zheng, J. Geophys. Res. **113**, B06204 (2008).
- 34 Y. G. G. Yu, Z. Q. Wu, and R. M. Wentzcovitch, Earth Planet. Sci. Lett. **273**, 115 (2008).
- 35 S. Baroni, S. de Gironcoli, A. Dal Corso, and P. Giannozzi, Rev. Mod. Phys. **73**, 515 (2001).
- 36 B. B. Karki, R. M. Wentzcovitch, S. de Gironcoli, and S. Baroni, Phys. Rev. B **61**, 8793 (2000).
- 37 Z. Q. Wu and R. M. Wentzcovitch, Phys. Rev. B **79**, 104304 (2009).
- 38 D. G. Isaak, O. L. Anderson, and T. Goto, Phys. Chem. Miner. **16**, 704 (1989).
- 39 C. daSilva, L. Stixrude, and R. M. Wentzcovitch, Geophys. Res. Lett. **24**, 1963 (1997).
- 40 L. Li, R. M. Wentzcovitch, D. J. Weidner, and C. R. S. Da Silva, J. Geophys. Res. **112**, B05206 (2007).
- 41 D. G. Isaak, O. L. Anderson, T. Goto, and I. Suzuki, Journal of Geophysical Research-Solid Earth and Planets **94**, 5895 (1989).
- 42 J. P. Poirier, *Introduction to the physics of the Earth's interior* (Cambridge University Press, 2000).

- <sup>43</sup> C. S. Zha, T. S. Duffy, R. T. Downs, H. K. Mao, and R. J. Hemley, J. Geophys.Res. **101**, 17535 (1996).
- <sup>44</sup> B. S. Li, J. Kung, and R. C. Liebermann, Physics of the Earth and Planetary Interiors **143-44**, 559 (2004).

## Figure Captions

**Figure 1.** Convention for azimuth angle.

**Figure 2.** (Color online) Relationship between strains in different coordinate systems. Structures before and after strains are applied are denoted in green and red, respectively. The structure experiences a shear strain as shown by the solid line if viewing from the  $X_1$  and  $X_2$  axis. This shear strain can also be viewed as a combination of a compressive strain along the  $X_1'$  and a tensile strain along the  $X_2'$  as indicated by the dashed lines.

**Figure 3.** (Color online) The temperature dependence of the elastic constant of MgO at 0 GPa (solid line), compared to results using the previous method<sup>11</sup> (the dashed lines) and experimental data<sup>38</sup> (open circles).

**Figure 4.** (Color online) The temperature dependence of the elastic modulus of forsterite at 0 GPa (solid line), compared to experimental data<sup>41</sup> (scatter points)

**Figure 5.** (Color online) The pressure dependence of the velocity of forsterite at various temperatures, compared with experiment data from Issak *et al.*<sup>41</sup> (open circles), Zha *et al.*<sup>43</sup> (solid circles) and Li *et al.*<sup>44</sup> (solid squares).

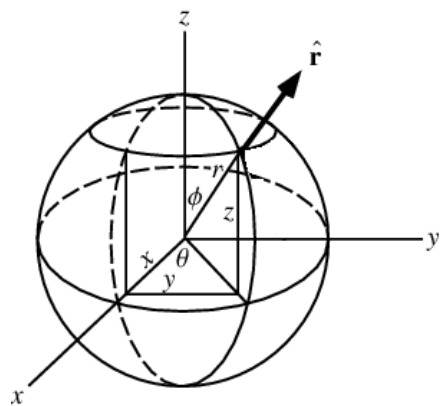


Fig. 1

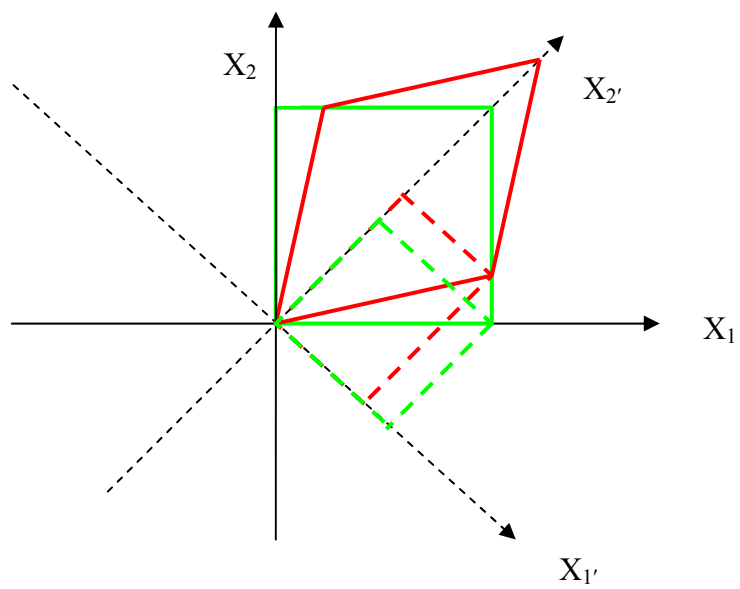


Fig .2



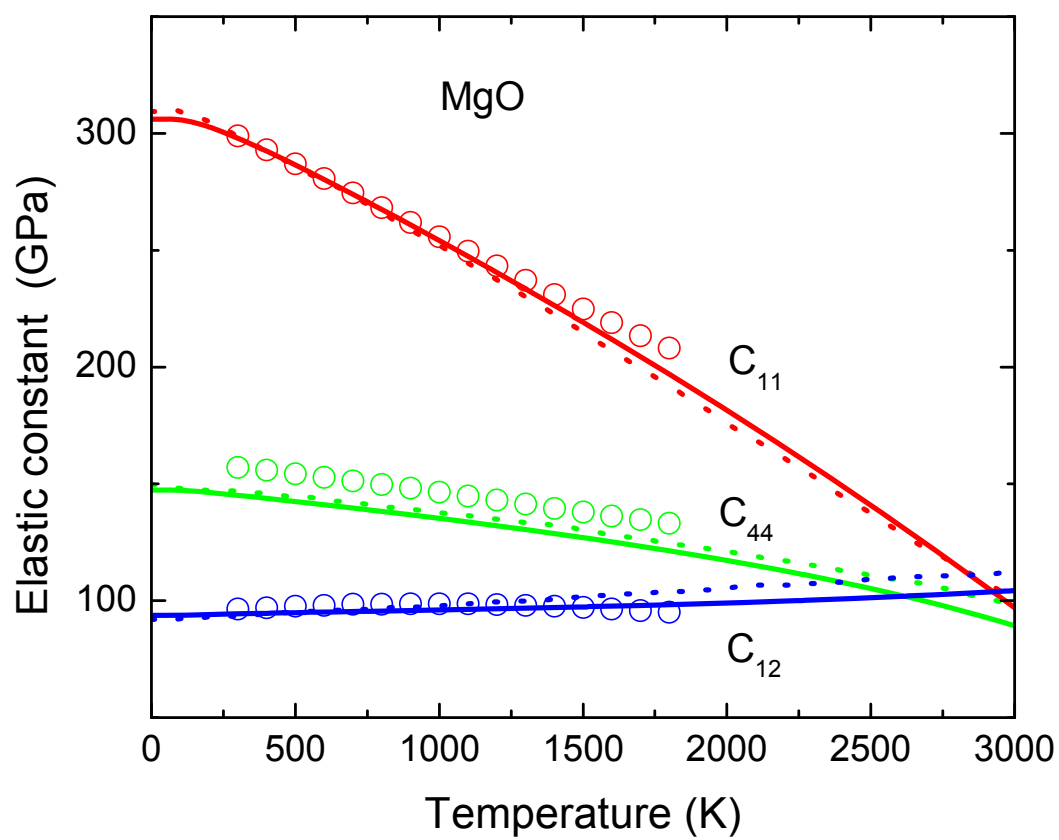


Fig. 3

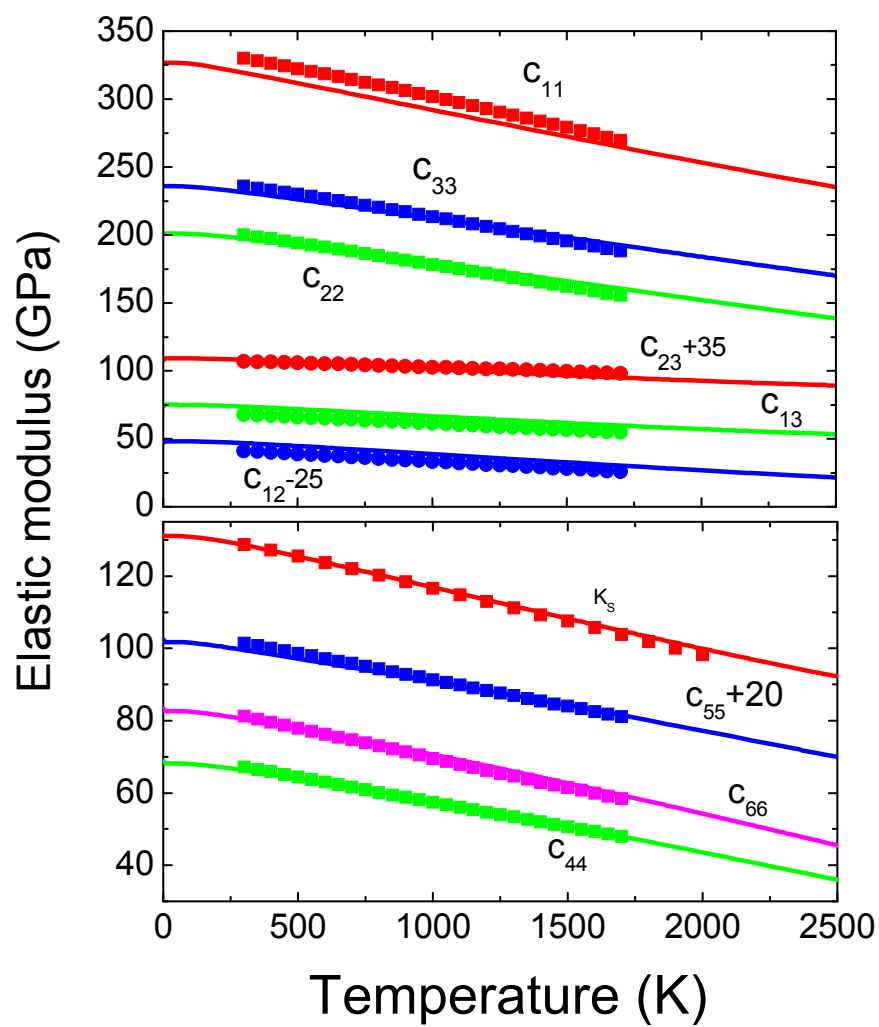


Fig. 4

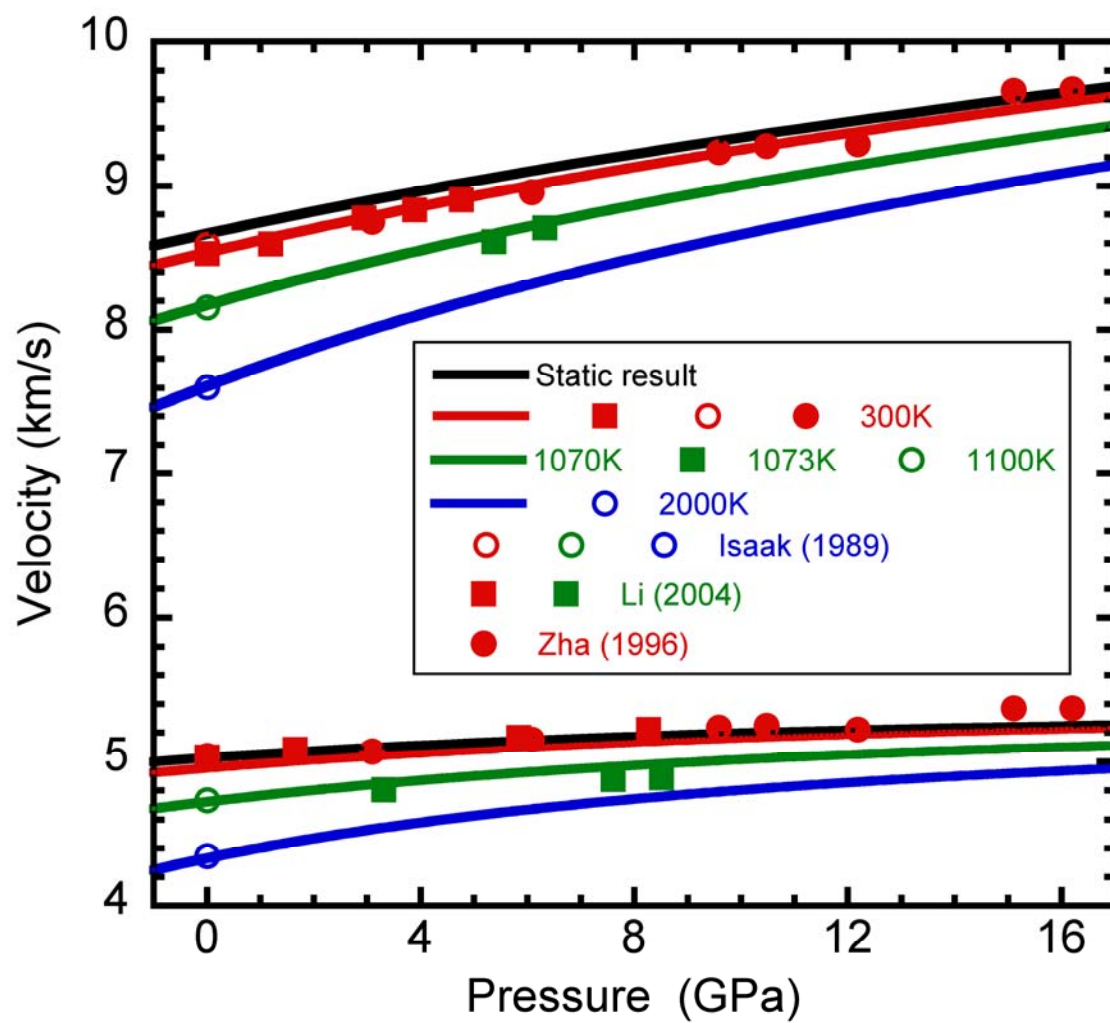


Fig. 5